| | Shrimp | | Pig | |
|---|---|---|---|---|
| | neutral | acid | neutral | acid |
| **α-helicity** | 0.411 +/- 0.021 | 0.498 +/- 0.021 | 0.332 +/- 0.019 | 0.500 +/- 0.022 |
| **Total Energy** | -7809.8 +/- 1010.8 | -5565.0 +/- 1010.8 | -2115.4 +/- 1010.8 | -422.8 +/- 1010.8 |
| Bond | 1720.6 +/- 35.6 | 1720.7 +/- 35.1 | 1690.3 +/- 34.6 | 1692.6 +/- 34.2 |
| Angle | 3066.7 +/- 58.8 | 3048.8 +/- 58.3 | 2866.4 +/- 53.1 | 3109.1 +/- 57.7 |
| VDW | -1978.3 +/- 43.1 | -2084.2 +/- 41.8 | -1942.9 +/- 42.3 | -2059.5 +/- 49.3 |
| Elec | -18335.2 +/- 758.2 | -16820.1 +/- 659.3 | -12133.2 +/- 752.7 | -11654.7 +/- 628.2 |

**Table S1: MD simulations of pig and shrimp Tpm under neutral and acidic conditions, Related to Figure 6.** Average α-helicity was specified as *i* to *i+4* backbone hydrogen bond occupancy. Total internal energy values with bonded (bond and angle) and non-bonded (van der Waals and electrostatic) terms were calculated as an average using the AMBER ff14SB force field.

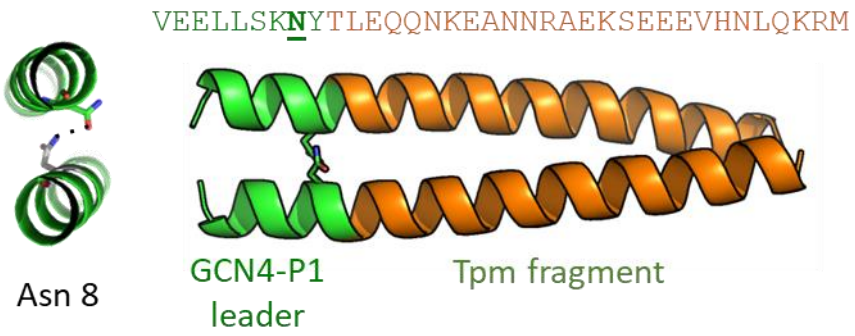


**Figure S1: Stabilizing Tpm peptides based on local sequence, Related to Star Methods.** Peptide design strategy is to add a GCN4-1 derived leader (VEELLSKNY, green) to the Tpm fragment (orange) with a core Asn-Asn hydrogen bond that constrains topology to a coiled-coil homodimer. This ensures that peptides derived from any Tpm sequence can produce its native structure.

**Table S2. Tpm fragment peptide sequences, Related to Star Methods and Key Resource Table.**

| *name* | *sequence* | *Tpm positions* |
|---|---|---|
| | **GCN4 Leader** **Tpm Fragment** | |
| S1 | Ac-VEELLSKNY AIKKKMQAMKLEKDNAMDRADTLEQQN-$NH_2$ | 3-29 |
| S2 | Ac-VEELLSKNY TLEQQNKEANNRAEKSEEEVHNLQKRM-$NH_2$ | 24-50 |
| S3 | Ac-VEELLSKNY KSEEEVHNLQKRMQQLENDLDQVQESL-$NH_2$ | 38-64 |
| S4 | Ac-VEELLSKNY QLENDLDQVQESLLKANIQLVEKDKAL-$NH_2$ | 52-78 |
| S5 | Ac-VEELLSKNY EKDKALSNAEGEVAALNRRIQLLEEDL-$NH_2$ | 73-99 |
| S6 | Ac-VEELLSKNY ALNRRIQLLEEDLERSEERLNTATTKL-$NH_2$ | 87-113 |
| S7 | Ac-VEELLSKNY RSEERLNTATTKLAEASQAADESERMR-$NH_2$ | 101-127 |
| S8 | Ac-VEELLSKNY VLENRSLSDEERMDALENQLKEARFLA-$NH_2$ | 129-155 |
| S9 | Ac-VEELLSKNY EARFLAEEADRKYDEVARKLAMVEADL-$NH_2$ | 150-176 |
| S10 | Ac-VEELLSKNY MVEADLERAEERAETGESKIVELEEEL-$NH_2$ | 171-197 |
| S11 | Ac-VEELLSKNY TGESKIVELEEELRVVGNNLKSLEVSE-$NH_2$ | 185-211 |
| S12 | Ac-VEELLSKNY VVGNNLKSLEVSEEKANQREEAYKEQI-$NH_2$ | 199-225 |
| S13 | Ac-VEELLSKNY TLTNKLKAAEARAEFAERSVQKLQKEV-$NH_2$ | 227-253 |
| S14 | Ac-VEELLSKNY RLEDELVNEKEKYKSITDELDQTFSEL-$NH_2$ | 255-281 |
| | | |
| P1 | Ac-VEELLSKNY AIKKKMQMLKLDKENALDRAEQAEADK-$NH_2$ | 3-29 |
| P2 | Ac-VEELLSKNY QAEADKKAAEDRSKRLEDELVSLQKKL-$NH_2$ | 24-50 |
| P3 | Ac-VEELLSKNY RLEDELVSLQKKLKATEDELDKYSEAL-$NH_2$ | 38-64 |
| P4 | Ac-VEELLSKNY ATEDELDKYSEAPKDAQEKLELAEKKA-$NH_2$ | 52-78 |
| P5 | Ac-VEELLSKNY LAEKKATDAEADVASLNRRIQLVEEEL-$NH_2$ | 73-99 |
| P6 | Ac-VEELLSKNY SLNRRIQLVEEELDRAQERLATALQKL-$NH_2$ | 87-113 |
| P7 | Ac-VEELLSKNY RAQERLATALQKLEEAEKAADESERGM-$NH_2$ | 101-127 |
| P8 | Ac-VEELLSKNY VIESRAQKDEEKMEIQEIQLKEAKHIA-$NH_2$ | 129-155 |
| P9 | Ac-VEELLSKNY EAKHIAEDADRKYEEVARKLVIIESDL-$NH_2$ | 150-176 |
| P10 | Ac-VEELLSKNY IIESDLERAEERAELSEGKCAELEEEL-$NH_2$ | 171-197 |
| P11 | Ac-VEELLSKNY LSEGKCAELEEELKTVTNNLKSLEAQA-$NH_2$ | 185-211 |
| P12 | Ac-VEELLSKNY TVTNNLKSLEAQAEKYSQKEDKYEEEI-$NH_2$ | 199-225 |
| P13 | Ac-VEELLSKNY VLSDKLKEAETRAEFAERSVTKLEKSI-$NH_2$ | 227-253 |
| P14 | Ac-VEELLSKNY DLEDELYAQKLKYKAISEELDHALNDM-$NH_2$ | 255-281 |

Ac N-terminal acetylation

-$NH_2$ C-terminal amidation

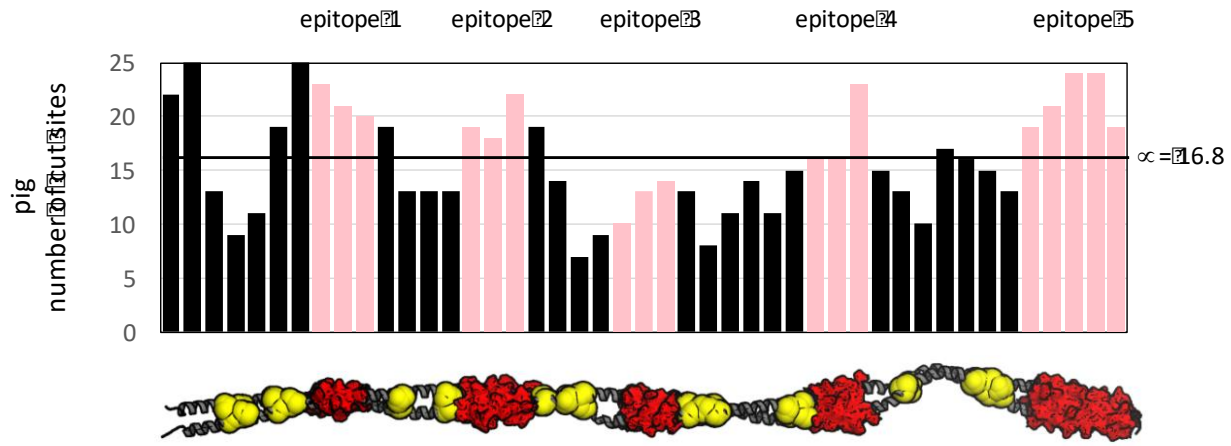


**Figure S2. Pig Tpm Proteoloysis, Related to Figure 6.** Number of pepsin, trypsin and chymotrypsin cleavage sites for 16-aa fragments of pig Tpm starting every six residues (i.e. 1-16, 7-22 …). Pink bars indicate fragments that overlap with sequence regions corresponding to epitopes from shrimp Tpm. Epitope-related regions are consistently above the mean number of cleavage sites (m = 16.8 sites / fragment).

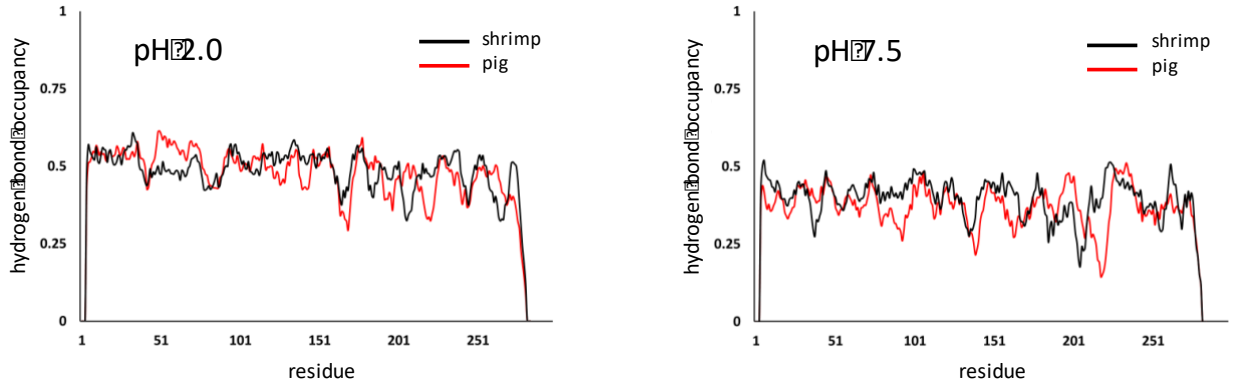


**Figure S3. Mean α-helicity for Tpm, Related to Figure 6.** MD production runs (70 ns) measured as *i*, *i+4* backbone amide – backbone carbonyl hydrogen bond occupancy (N-O distance < 3.0Å, N-H-O angle > 135º).

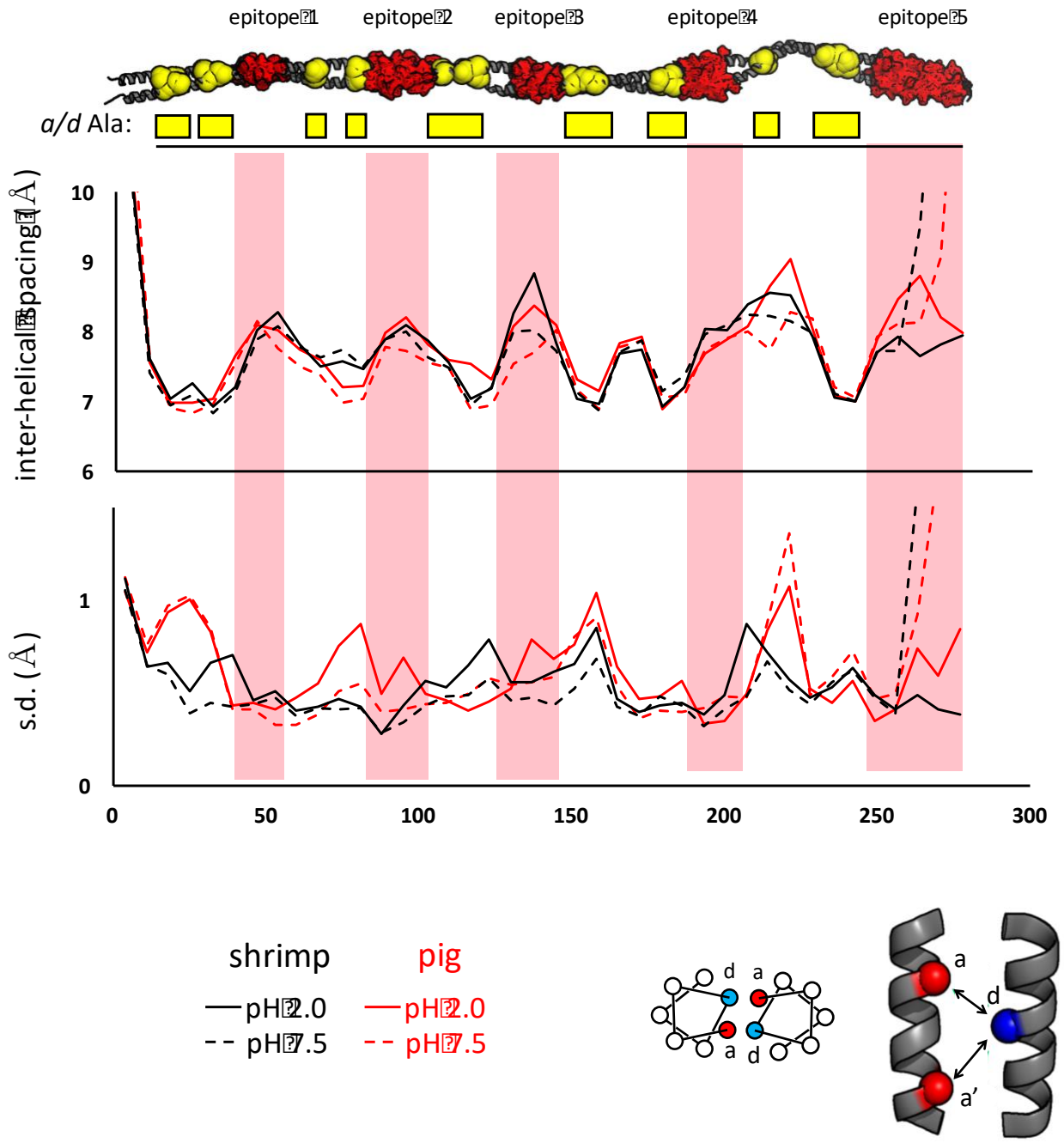


**Figure S4. MD analysis of local and global Tpm dynamics, Related to Figure 6.** Epitopes (red) and *a* or *d* heptad position Ala-clusters (yellow) highlighted on a model of the Tpm coiled coil. Interhelical spacing is calculated between the *d* position on one chain and the *a* and *a'* positions on the neighboring chain as (*da* + *da'*)/2. Mean interhelical spacing and standard deviation of spacing are shown for both shrimp and pig Tpm molecular dynamics trajectories at acid and neutral pH.

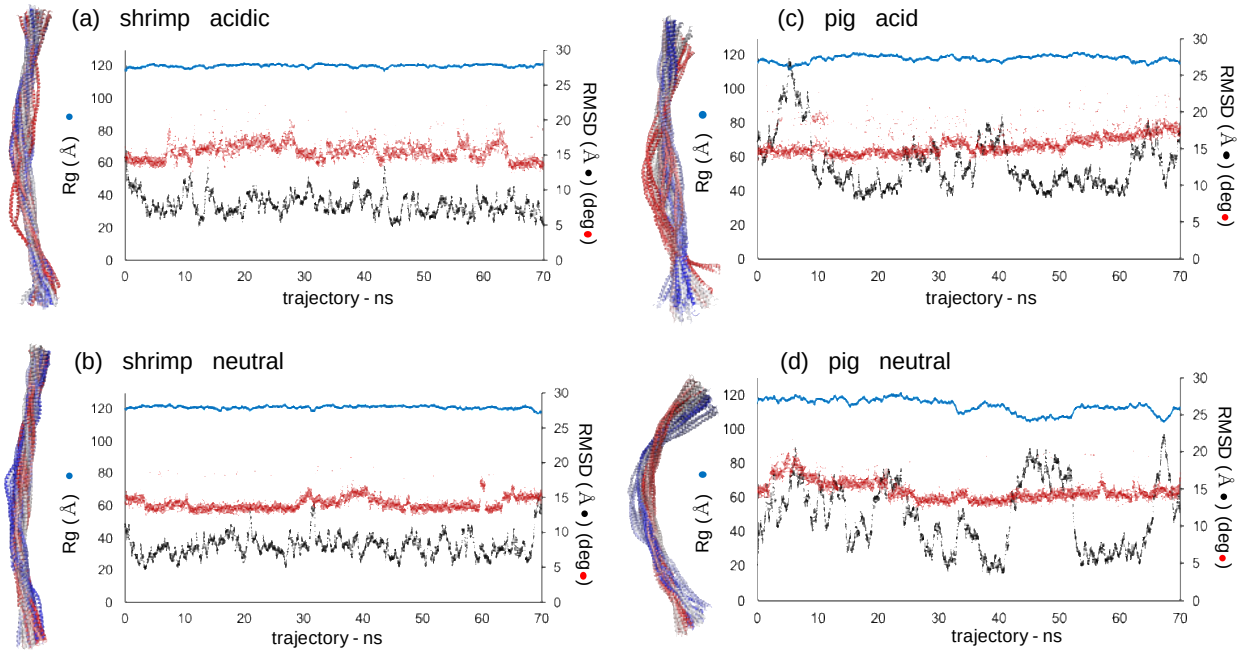


**Figure S5. Global descriptors of Tpm conformational dynamics, Related to Figure 7.** Radius of gyration (Rg) and Cartesian RMSD are computed using Cα positions only. Angular RMSD based on backbone phi and psi torsions.

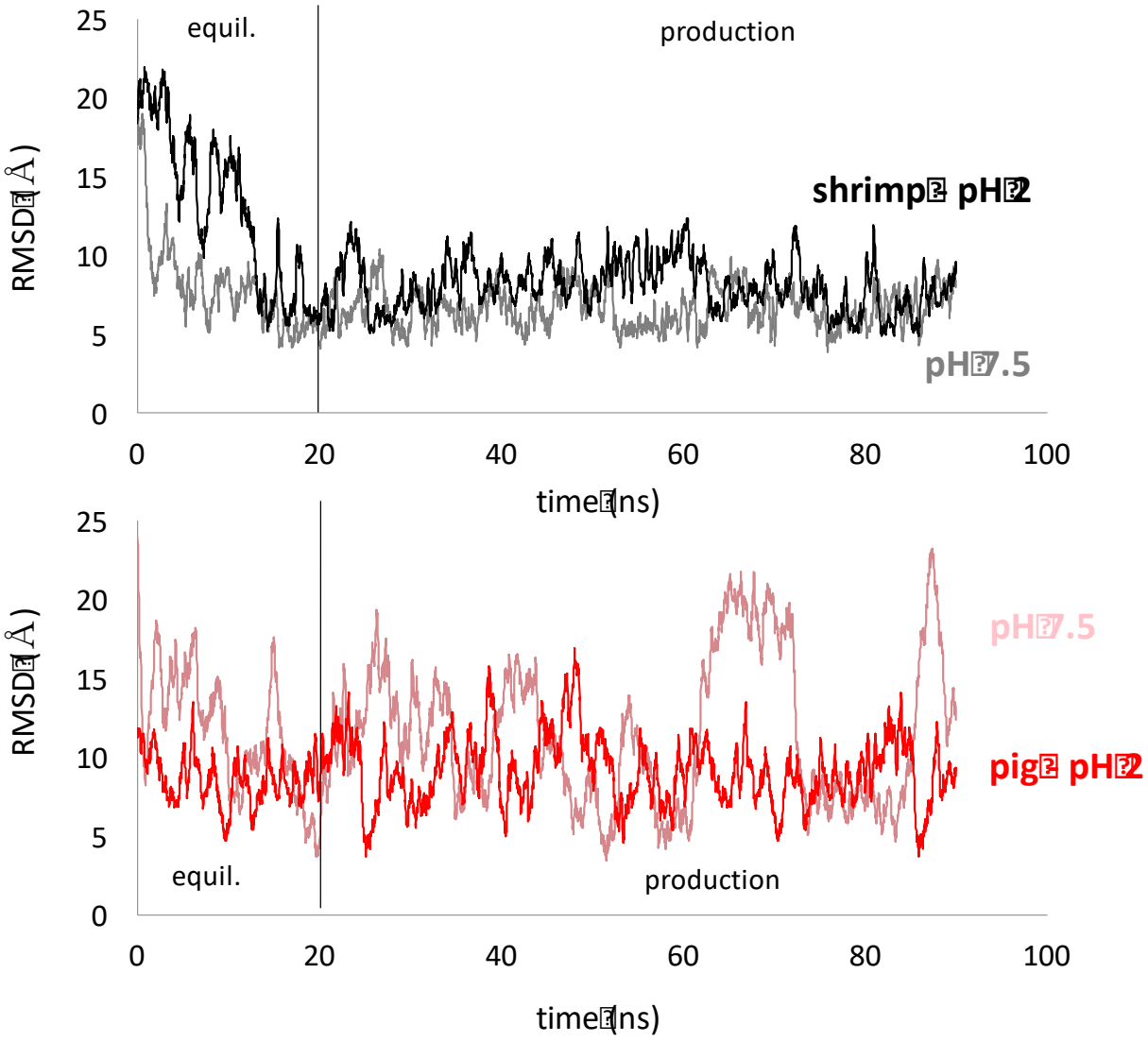


**Figure S6. RMSD of entire trajectories for shrimp and pig Tpm and acidic and neutral pH, Related to Star Methods and Figures 6, 7.** The 70 ns production run starts after a 20 ns equilibration phase.